



ChemComm

**Disproportionation of  $\text{Sn(II)}\{\text{CH}(\text{SiMe}_3)_2\}_2$  to  
 $\cdot\text{Sn(III)}\{\text{CH}(\text{SiMe}_3)_2\}_3$  and  $\cdot\text{Sn(I)}\{\text{CH}(\text{SiMe}_3)_2\}$ :  
Characterization of the Sn(I) Product**

Journal:	<i>ChemComm</i>
Manuscript ID	CC-COM-03-2023-001542.R1
Article Type:	Communication

SCHOLARONE™  
Manuscripts

## COMMUNICATION

## Disproportionation of $\text{Sn(II)}\{\text{CH}(\text{SiMe}_3)_2\}_2$ to $\cdot\text{Sn(III)}\{\text{CH}(\text{SiMe}_3)_2\}_3$ and $\cdot\text{Sn(I)}\{\text{CH}(\text{SiMe}_3)_2\}$ : Characterization of the $\text{Sn(I)}$ product

Received 00th January 20xx,  
Accepted 00th January 20xx

Kristian L. Mears,<sup>a</sup> Bronson Ruiz,<sup>a†</sup> Gia-Ann Nguyen,<sup>a†</sup> Wenxing Zou,<sup>a</sup> James C. Fettinger,<sup>a</sup> and Philip P. Power<sup>\*a</sup>

DOI: 10.1039/x0xx00000x

Half a century since the photolytic disproportionation of Lappert's dialkyl stannylene  $\text{SnR}_2$ ,  $\text{R} = \text{CH}(\text{SiMe}_3)_2$  (**1**) gave the persistent trivalent radical  $[\cdot\text{SnR}_3]$ , the characterization of the corresponding  $\text{Sn(I)}$  product,  $\cdot\text{SnR}$  is now described. It was isolated as the hexastannaprismane  $\text{Sn}_6\text{R}_6$  (**2**), from the reduction of **1** by the  $\text{Mg(I)}$ -reagent,  $\text{Mg}(\text{BDI}^{\text{Dip}})_2$  ( $\text{BDI} = (\text{DipNCMe})_2\text{CH}$ ,  $\text{Dip} = 2,6$ -diisopropylphenyl).

In 1973,<sup>1,2</sup> Lappert and coworkers reported the generation of the first long-lived tin(III) radical<sup>3–5</sup> via the irradiation of the dialkylstannylene  $\text{Sn}\{\text{CH}(\text{SiMe}_3)_2\}_2$  (**1**) in solution by ambient visible light. This generated a remarkably persistent<sup>2</sup>  $\cdot\text{Sn}\{\text{CH}(\text{SiMe}_3)_2\}_3$  radical. It was proposed that this arose from the disproportionation  $2 \text{Sn}^{\text{II}}\{\text{CH}(\text{SiMe}_3)_2\}_2 \rightleftharpoons \cdot\text{Sn}^{\text{III}}\{\text{CH}(\text{SiMe}_3)_2\}_3 + \cdot\text{Sn}^{\text{I}}\{\text{CH}(\text{SiMe}_3)_2\}$  (Fig. 1, top). The  $\cdot\text{Sn}^{\text{III}}\{\text{CH}(\text{SiMe}_3)_2\}_3$  radical was characterized by electron spin resonance (ESR) spectroscopy, but its  $\text{Sn(I)}$  partner, the tin(I) radical  $\cdot\text{Sn}\{\text{CH}(\text{SiMe}_3)_2\}$  has never been characterized. Despite the proposed mechanism of  $\text{Sn-C}$  bond cleavage followed by  $\cdot\text{CH}(\text{SiMe}_3)_2$  addition to another molecule of the dialkylstannylene **1** acting as a spin trap to generate  $\cdot\text{Sn}\{\text{CH}(\text{SiMe}_3)_2\}_3$ , no decomposition products or other radical-source (e.g.  $(\text{tBuON})_2$  or azobisisobutyronitrile) trapped products were isolated.<sup>6</sup> In related investigations, the isoelectronic tin(II) amide  $\text{Sn}\{\text{N}(\text{SiMe}_3)_2\}_2$ ,<sup>7–10</sup> was also shown to disproportionate photochemically to the tris-amido tin(III) radical  $\cdot\text{Sn}\{\text{N}(\text{SiMe}_3)_2\}_3$ ,<sup>10,11</sup> but the corresponding isoelectronic radical tin(I) amide has also remained elusive. Since then, the chemistry of tin radicals stabilized by sterically bulky ligands has received much attention, both computationally<sup>12,13</sup> and experimentally.<sup>14–17</sup> For example, the distannyne  $\text{Ar}^{\text{iPr}_4}\text{SnSnAr}^{\text{iPr}_4}$ ,  $\text{Ar}^{\text{iPr}_4} = \text{C}_6\text{H}_3\text{-}2,6(\text{C}_6\text{H}_3\text{-}2,6\text{-iPr}_2)_2$  undergoes

reversible cleavage in solution to afford two one-coordinate  $\text{Sn(I)} : \text{SnAr}^{\text{iPr}_4}$  radicals (which exist in equilibrium with its corresponding distannyne dimer).<sup>15</sup> More recently, the isolation of a tin radical anion<sup>18</sup> and a neutral one-coordinate tin<sup>19</sup> radical has been reported by Hicks and Tan respectively.

Tin radicals in solution<sup>20</sup> and particularly low-coordinate radicals, often undergo self-radical trapping leading to cluster formation.<sup>21</sup> A variety of examples in the literature have shown that even bulky aryl or terphenyl ligands at the tin atom can be insufficiently bulky to prevent the formation of clusters,<sup>22–24</sup> or metalloid clusters.<sup>25–27</sup> Consideration of the absence of an ESR signal for Lappert's tin(I) alkyl radical  $\cdot\text{Sn}\{\text{CH}(\text{SiMe}_3)_2\}$ , leads to the notion of a rapid formation of a self-trapped cluster with formula  $1/n[\text{Sn}_n\text{R}_n]$ . A synthetic route towards the isolation of such a compound might be easier than photochemical disproportionation. Schulz and coworkers showed that a metalloid tin cluster featuring 2,4,6-triisopropylphenyl (Trip) ligands of formula  $\text{Sn}_{10}\{\text{Trip}\}_8$  could be accessed by the reduction of the parent distannene,<sup>25,28–30</sup>  $\text{Sn}_2(\text{Trip})_4$  using Jones' magnesium(I) reductants<sup>31</sup> at high temperature, which also produced the kinetically stabilized insertion product,  $[\text{BDI}^{\text{Dip}}\text{Mg}(\text{Trip})]$ ,  $\text{BDI} = (\text{DipNCMe})_2\text{CH}$ ,  $\text{Dip} = 2,6$ -diisopropylphenyl).

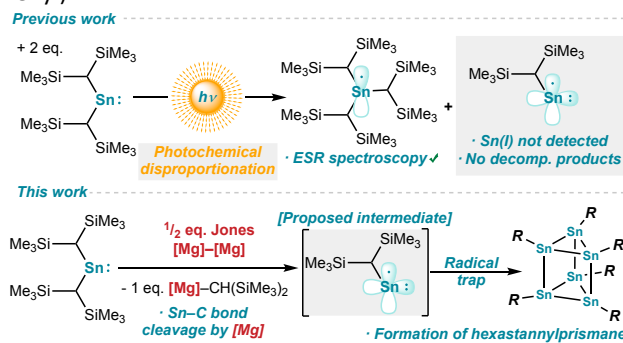


Fig. 1. Overview of the previous work carried out by Lappert and coworkers (top) and the work reported here.  $\text{R} = \text{CH}(\text{SiMe}_3)_2$ .

<sup>a</sup> Department of Chemistry, One Shields Avenue, Davis, University of California, 95616, USA. † These authors contributed equally.

Electronic Supplementary Information (ESI) available: [Experimental details, NMR and UV-Vis spectra and other details]. See DOI: 10.1039/x0xx00000x

Here, we report the route to a hexastannaprismane of the formula  $\text{Sn}_6(\text{CH}(\text{SiMe}_3)_2)_6$ , cluster **2** (Fig. 1, bottom). The isolation, structural and spectroscopic characterization of this cluster provides evidence for the formation of a one-coordinate Lappert alkyl tin(I) radical, half a century after the initial report. The synthesis of cluster **2** was carried out according to Fig. 2, Scheme 1, where 6 equivalents of the alkyl stannylene (complex **1**) was combined with 3 equivalents of the magnesium(I) dimer  $\{\text{Mg}(\text{BDI}^{\text{Dip}})\}_2$ ,  $\text{BDI} = (\text{DipNCMe})_2\text{CH}$ ,  $\text{Dip} = 2,6$ -diisopropylphenyl<sup>31</sup> in 10 mL of toluene at room temperature. The solution immediately became an intense red/pink color and was stirred for a further 12 hours. Unlike Schulz's report, elevated temperatures were not required for the conversion of **1** to **2**, likely the result of the bonding and lower coordination at the Sn atom in **1** vs those in the distannene  $\text{Sn}_2(\text{Trip})_4$ . After 12 hours, a colorless precipitate had formed, which was separated from the red solution by filtration. Storage of the red filtrate at  $-30^\circ\text{C}$  overnight yielded cluster **2** as intensely colored red-orange crystals (SI) that were suitable for single crystal X-ray diffraction analysis (Fig. 2).

Scheme 1

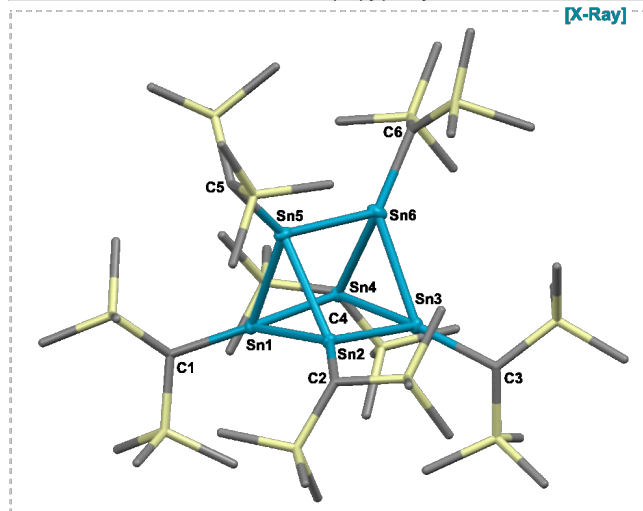
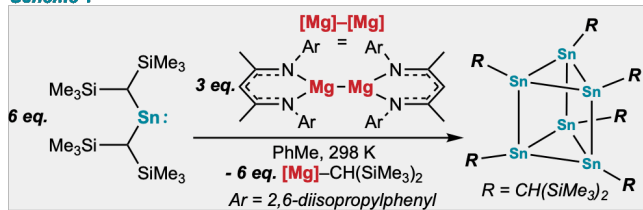


**Fig. 2.** Top: Synthetic route to  $\text{Sn}_6(\text{CH}(\text{SiMe}_3)_2)_6$  (**2**). Bottom: Molecular structure of **2** (hydrogens are not shown). Sn = blue, C = grey and Si = yellow. Selected bond lengths (Å) include: Sn1–Sn2 = 2.8670(4), Sn2–Sn3 = 2.8162(4), Sn3–Sn4 = 2.9255(4), Sn4–Sn1 = 2.8328(4), Sn5–Sn6 = 2.8290(4), Sn1–Sn5 = 2.9153(3), Sn2–Sn5 = 2.9013(4), Sn3–Sn6 = 2.8751(4), Sn4–Sn6 = 2.9027(3). Selected bond angles ( $^\circ$ ) include: Sn1–Sn5–Sn2 = 60.226(9), Sn1–Sn2–Sn3 = 87.448(11), Sn3–Sn6–Sn5 = 92.900(11).

The X-ray analysis reveals that cluster **2** has a trigonal prismatic structure, with an average Sn–Sn bond length of 2.8573(4) Å, with the shortest between Sn2–Sn3 = 2.8162(4) Å and the longest between Sn3–Sn4 = 2.9255(4) Å. The distance between the center of the two triangular faces (plane centroid–plane centroid, Fig S10, SI) is 2.817 Å, with a twist angle of 7.566°, likely to accommodate the bulky  $-\text{CH}(\text{SiMe}_3)_2$  ligands. There is

no significant difference between the Sn–Sn lengths within each triangle face and the Sn–Sn lengths between the triangle faces (Fig 3). The greatest Sn–Sn distance lies diagonally across the prism between Sn5–Sn3 = 4.134 Å, which is much longer than the sum of the covalent radii (2.80 Å)<sup>32</sup> and slightly shorter than the sum of the van der Waals radii of 4.34 Å.<sup>33</sup> The bond angles between the vertices, for example between Sn1, Sn2 and Sn5 confirm a regular triangular prism, which include Sn1–Sn5–Sn2 = 60.226(9)°, Sn1–Sn2–Sn5 = 60.172(9)° and Sn5–Sn1–Sn2 = 59.062(9)°.

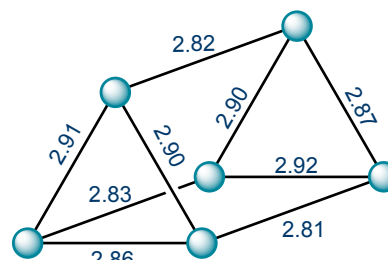


**Fig. 3.** Schematic drawing of the  $\text{Sn}_6$  core **2** in the same orientation as Fig. 2, including the bond lengths (Å) between the Sn vertices.

When compared to Schulz's metalloid cluster  $[\text{Sn}_{10}\text{Trip}_8]$  which displayed a distorted butterfly structure, the shortest Sn–Sn bond distance was found to be 2.8069(9) Å, which is crystallographically distinguishable ( $>3\sigma$ ) from the shortest Sn–Sn distance in complex **2**. Only two other examples of  $\text{Sn}_6$  clusters with this type of structure are known, Wiberg's hexasupersilyl-triprismo-hexastannane  $\text{Sn}_6\{\text{Si}^t\text{Bu}_3\}_6$ ,<sup>34</sup> and Jones' distorted trigonal anti-prismatic hexaamido-hexastannane  $\text{Sn}_6\{\text{N}^t\text{Bu}(\text{Dip})\}_6$  (Fig. 4).<sup>35</sup>

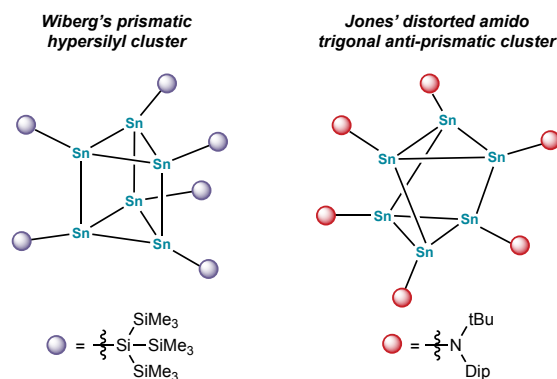


**Fig. 4.** Previous examples of tin clusters with similar geometries to **2**. Left: Wiberg's  $\text{Sn}_6\{\text{Si}^t\text{Bu}_3\}_6$  cluster.<sup>34</sup> Right: Jones'  $\text{Sn}_6\{\text{N}^t\text{Bu}(\text{Dip})\}_6$ , Dip = 2,6-diisopropylphenyl.<sup>35</sup>

Compared to these (Fig. 3), **2** has the shortest Sn–Sn bond length of the series and is significantly shorter those in Wiberg's<sup>34</sup> and Jones'<sup>33,35</sup> examples (2.903(1) Å and 2.9693(12) Å respectively). Of the longest Sn–Sn bond lengths in these clusters, complex **2** also displays the shortest Sn–Sn distance of 2.9255(4) Å, in comparison to 2.941(1) Å (Wiberg) and 3.2825(11) Å (Jones). The geometry of complex **2** is similar to that of the Wiberg cluster, which both feature slightly distorted trigonal prismatic geometry, which likely results from

lower strain within the framework in comparison to an octahedral cluster, as the angles within an octahedron are narrower than in the trigonal prismatic geometry adopted by **2**.<sup>36</sup>

There are several close H⋯H contacts within the structure (SI, Fig S11) that are shorter than the sum of the van der Waals radii (2.4 Å) between the protons of the SiMe<sub>3</sub> ligands (from adjacent Sn vertices) that likely contribute to a stabilization effect through dispersion interactions.<sup>37</sup>

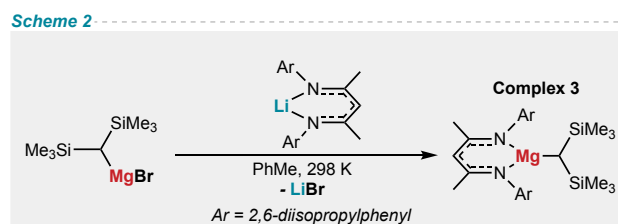
The UV-Vis spectrum of **2** shows a  $\lambda_{\text{max}} = 353 \text{ nm}$  (3.4 eV, 80.2 kcal mol<sup>-1</sup>) which is likely due to a HOMO-LUMO transition, as well as a broad shoulder at 496 nm (2.4 eV, 56.6 kcal mol<sup>-1</sup>). These absorptions are bathochromically shifted ( $\Delta\lambda_{\text{max}} = 21 \text{ nm}$ ) when compared to the transitions displayed for stannylene **1**.<sup>3</sup> The <sup>1</sup>H NMR spectrum shows the expected signals for the -CHSiMe<sub>3</sub> and -CHSiMe<sub>3</sub> protons at  $\delta = 0.21 \text{ ppm}$  and  $\delta = 0.36 \text{ ppm}$  respectively. These signals are slightly shifted compared to those in the stannylene (**1**) which appeared at  $\delta = 0.32 \text{ ppm}$  and  $\delta = 1.90 \text{ ppm}$  respectively.<sup>3</sup> The frustrated rotational motion of the SiMe<sub>3</sub> groups give rise to a second signal at  $\delta = 0.40 \text{ ppm}$ . This process is also evidenced in the <sup>13</sup>C{<sup>1</sup>H} NMR, with 2 peaks for the -CHSiMe<sub>3</sub> carbons at  $\delta = 4.01$  and 3.91 ppm, and the -CHSiMe<sub>3</sub> is further upfield at  $\delta = 1.43 \text{ ppm}$ . <sup>29</sup>Si NMR spectroscopy displayed two signals at  $\delta = -2.10$  and  $\delta = -6.19 \text{ ppm}$  in the ratio of 1:2 respectively, confirming that two of the six -CH(SiMe<sub>3</sub>)<sub>2</sub> ligands are in slightly different chemical environments. Weak <sup>2</sup>J(<sup>29</sup>Si-<sup>1</sup>H) coupling was observed for the more intense peak at  $\delta = -6.19 \text{ ppm}$  with a coupling constant of 5.5 Hz.

<sup>1</sup>H DOSY NMR spectroscopy confirmed that these peaks correspond to the same species (cluster **2**) in solution, with a diffusion coefficient of  $4.11 \times 10^{-10} \text{ m}^2 \text{ s}^{-1}$ . Calculating the hydrodynamic radius (SI) of **2** in benzene affords an approximated spherical radius of 7.67 Å, which is in excellent agreement to the radius calculated from the volume of the single crystal X-ray data (7.69 Å) and further shows that **2** remains a cluster in solution.

A single <sup>119</sup>Sn NMR signal is displayed at  $\delta = +225.9 \text{ ppm}$  (scan width = +3500 to -550 ppm), indicating magnetic equivalence of all Sn atoms, and displays very weak <sup>1</sup>J(<sup>119</sup>Sn-<sup>117</sup>Sn) coupling (210.7 Hz). This signal is shifted far upfield from other stannylenes,<sup>38,39</sup> due to the greater shielding effect of the 6-Sn core, (for example, **1** displays a <sup>119</sup>Sn NMR signal at  $\delta = +2328 \text{ ppm}$ ).<sup>40</sup> Similar <sup>119</sup>Sn NMR signals have been observed for clusters including Schulz's Sn<sub>10</sub>(Trip)<sub>8</sub>, for which 3 individual <sup>119</sup>Sn signals were observed at  $\delta = +358.9$ , +236.7 and +134.7 ppm, indicating magnetically inequivalent Sn atoms within the structure. The clusters Sn<sub>7</sub>{C<sub>6</sub>H<sub>3</sub>-2,6-(C<sub>6</sub>H<sub>3</sub>-2,6-iPr<sub>2</sub>)<sub>2</sub>}<sup>20</sup> and Sn<sub>8</sub>{C<sub>6</sub>H<sub>3</sub>-2,6-(C<sub>6</sub>H<sub>2</sub>-2,4,6-Me<sub>3</sub>)<sub>4</sub>}<sup>23,41</sup> display signals at  $\delta = +419.5$ , +529.7 ppm and  $\delta = +483.1$ , +751.7 ppm respectively.

Complex **3**, [BDI<sup>Dip</sup>Mg(CH(SiMe<sub>3</sub>)<sub>2</sub>)] was identified from the <sup>1</sup>H NMR spectrum of the reaction mixture during the synthesis of **2**. The <sup>1</sup>H NMR spectrum showed the typical methine proton of the BDI<sup>Dip</sup> ligand had shifted to  $\delta = 4.83 \text{ ppm}$  (from  $\delta = 4.87 \text{ ppm}$  in the Mg(I) reagent),<sup>31</sup> and an expected upfield signal for the BDI<sup>Dip</sup>Mg-CH(SiMe<sub>3</sub>)<sub>2</sub> proton ( $\delta = -1.59 \text{ ppm}$ ). For improved

analysis, complex **3** could also be synthesized directly (Scheme 2).



Scheme 2: Alternative synthetic route towards complex **3**.

In conclusion, we have found after 50 years, that the isolation and structural characterization of the Sn(I) product that was proposed to form in the disproportionation of Lappert's dialkyl stannylene, :Sn{CH(SiMe<sub>3</sub>)<sub>2</sub>}<sub>2</sub> can be afforded readily. The product was isolated as a self-trapped cluster of the formula Sn<sub>6</sub>{CH(SiMe<sub>3</sub>)<sub>2</sub>}<sub>6</sub> (**2**) which adopts a trigonal prismatic structure and displays an upfield <sup>119</sup>Sn NMR signal of  $\delta = +225.9 \text{ ppm}$ . Experiments to characterize the isoelectronic Lappert amide Sn(I) analogue from Sn{N(SiMe<sub>3</sub>)<sub>2</sub>}<sub>2</sub> are currently underway.

## Acknowledgements

We thank the U.S. National Science Foundation for funding (Grant No. CHE-2152760) and for the purchase of a dual-source X-ray diffractometer (Grant No. CHE-1531193).

## Conflicts of interest

There are no conflicts to declare.

## Notes and references

- 1 B. J. Peter Davidson and M. F. Lappert, *J. Chem. Soc. Chem. Comm.*, 1973, 317a–317a.
- 2 P. J. Davidson, A. Hudson, M. F. Lappert and P. W. Lednor, *J. Chem. Soc. Chem. Comm.*, 1973, **21**, 829–830.
- 3 P. J. Davidson, D. H. Harris and M. F. Lappert, *J. Chem. Soc. Dalton Trans.*, 1976, 2268–2274.
- 4 D. E. Goldberg, D. H. Harris, M. F. Lappert and K. M. Thomas, *J. Chem. Soc. Chem. Comm.*, 1976, **7**, 261–262.
- 5 J. D. Cotton, P. J. Davidson and M. F. Lappert, *J. Chem. Soc. Dalton Trans.*, 1976, 2275–2286.
- 6 A. Hudson, M. F. Lappert and P. W. Lednor, *J. Chem. Soc. Dalton Trans.*, 1976, **22**, 2369–2375.
- 7 D. H. Harris and M. F. Lappert, *J. Chem. Soc., Chem. Comm.*, 1974, **21**, 895–896.

## COMMUNICATION

## Journal Name

- 8 M. F. Lappert and P. P. Power, in *Organotin Compounds: New Chemistry and Applications*, 1976, vol. 8, pp. 70–81. 27 C. P. Sindlinger and L. Wesemann, *Chem. Sci.*, 2014, **5**, 2739–2746.
- 9 M. F. Lappert, P. P. Power, M. J. Slade, L. Hedberg, K. Hedberg and V. Schomaker, *J. Chem. Soc., Chem. Comm.*, 1979, **8**, 369–370. 28 S. Masamune and L. R. Sita, *J. Am. Chem. Soc.*, 1985, **107**, 6390–6391.
- 10 M. S. Gynane, D. H. Harris, M. F. Lappert, P. P. Power, P. Riviere and M. Riviere-Baudet, *J. Chem. Soc., Dalton Trans.*, 1977, **20**, 2004–2009. 29 S. Masamune, L. R. Sita and D. J. Williams, *J. Am. Chem. Soc.*, 1983, **105**, 630–631.
- 11 J. D. Cotton, C. S. Cundy, D. H. Harris, A. Hudson, M. F. Lappert and P. W. Lednor, *J. Chem. Soc., Chem. Comm.*, 1974, **16**, 651–652. 30 W. Zou, M. Bursch, K. L. Mears, C. Stennett, P. Yu, J. Fettinger, S. Grimme and P. P. Power, *Angew. Chem. Int. Ed.*, 2023, e202301919.
- 12 L. Broeckaert, J. Turek, R. Olejník, A. Růžička, M. Biesemans, P. Geerlings, R. Willem and F. De Proft, *Organometallics*, 2013, **32**, 2121–2134. 31 S. P. Green, C. Jones and A. Stasch, *Science (1979)*, 2007, **318**, 1754–1757.
- 13 R. Sedlak, O. A. Stasyuk, C. Fonseca Guerra, J. Řezáč, A. Růžička and P. Hobza, *J. Chem. Theory Comp.*, 2016, **12**, 1696–1704. 32 P. Pyykkö and M. Atsumi, *Chem. Eur. J.*, 2009, **15**, 186–197.
- 14 T. Y. Lai, J. C. Fettinger and P. P. Power, *J. Am. Chem. Soc.*, 2018, **140**, 5674–5677. 33 M. Mantina, A. C. Chamberlin, R. Valero, C. J. Cramer and D. G. Truhlar, *J. Phys. Chem. A.*, 2009, **113**, 5806–5812.
- 15 T. Y. Lai, L. Tao, R. D. Britt and P. P. Power, *J. Am. Chem. Soc.*, 2019, **141**, 12527–12530. 34 N. Wiberg, H.-W. Lerner, H. Nöth and W. Ponikvar, *Angew. Chem. Int. Ed.*, 1999, **38**, 1103–1105.
- 16 V. Y. Lee and A. Sekiguchi, in *Organometallic Compounds of Low-Coordinate Si, Ge, Sn and Pb: From Phantom Species to Stable Compounds*, John Wiley and Sons, 2010, chapter 2. 35 J. A. Kelly, M. Juckel, T. J. Hadlington, I. Fernández, G. Frenking and C. Jones, *Chem. Eur. J.*, 2019, **25**, 2773–2785.
- 17 A. Sekiguchi, T. Fukawa, V. Y. Lee and M. Nakamoto, *J. Am. Chem. Soc.*, 2003, **125**, 9250–9251. 36 A. F. Richards, H. Hope and P. P. Power, *Angew. Chem. Int. Ed.*, 2003, **42**, 4071–4074.
- 18 L. F. Lim, M. Judd, P. Vasko, M. G. Gardiner, D. A. Pantazis, N. Cox and J. Hicks, *Angew. Chem. Int. Ed.*, 2022, **134**, e202201248. 37 K. L. Mears and P. P. Power, *Acc. Chem. Res.*, 2022, **55**, 1337–1348.
- 19 D. Wang, W. Chen, C. Zhai, L. Zhao, S. Ye and G. Tan, *J. Am. Chem. Soc.*, DOI:10.1021/JACS.3C00421. 38 R. J. Schwamm, C. A. von Randow, A. Mouchfiq, M. J. Evans, M. P. Coles and J. Robin Fulton, *Eur. J. Inorg. Chem.*, 2021, **34**, 3466–3473.
- 20 P. P. Power, *Chem. Rev.*, 2003, **103**, 789–809. 39 V. Y. Lee, T. Fukawa, M. Nakamoto, A. Sekiguchi, B. L. Tumanskii, M. Karni and Y. Apeloig, *J. Am. Chem. Soc.*, 2006, **128**, 11643–11651.
- 21 N. Wiberg and P. P. Power, in *Molecular Clusters of the Main Group Elements*, John Wiley & Sons, Ltd, 2005, pp. 188–208. 40 K. W. Zilm, G. A. Lawless, R. M. Merrill, J. M. Millar and G. G. Webb, *J. Am. Chem. Soc.*, 1987, **109**, 7236–7238.
- 22 M. Brynda, R. Herber, P. B. Hitchcock, M. F. Lappert, I. Nowik, P. P. Power, A. V. Protchenko, A. Růžička and J. Steiner, *Angew. Chem. Int. Ed.*, 2006, **118**, 4439–4443. 41 E. Rivard, J. Steiner, J. C. Fettinger, J. R. Giuliani, M. P. Augustine and P. P. Power, *Chem. Commun.*, 2007, **46**, 4919–4921.
- 23 B. E. Eichler and P. P. Power, *Angew. Chem. Int. Ed.*, 2001, **40**, 796–797.
- 24 J. J. Maudrich, C. P. Sindlinger, F. S. W. Aicher, K. Eichele, H. Schubert and L. Wesemann, *Chem. Eur. J.*, 2017, **23**, 2192–2200.
- 25 J. Wiederkehr, C. Wölper and S. Schulz, *Chem. Commun.*, 2016, **52**, 12282–12285.
- 26 L. R. Sita, *Acc. Chem. Res.*, 1994, **27**, 191–197.